Lipid interaction of *Pseudomonas aeruginosa* exotoxin A

Acid-triggered permeabilization and aggregation of lipid vesicles

Gianfranco Menestrina,* Cecilia Pederzolli,‡ Stefano Forti,‡ and Franco Gambale§

*Dipartimento di Fisica, Universita' di Trento, I-38050 Povo (Trento), Italy; ‡Istituto per la Ricerca Scientifica e Tecnologica, Via alla Cascata, I-38050 Povo (Trento), Italy; and §Istituto di Cibernetica e Biofisica and Dipartimento di Fisica, Universita' di Genova, I-16146 Genova, Italy

ABSTRACT We have investigated the interaction of *Pseudomonas* exotoxin A with small unilamellar vesicles comprised of different phospholipids as a function of pH, toxin, and lipid concentration. We have found that this toxin induces vesicle permeabilization, as measured by the release of a fluorescent dye. Permeabilization is due to the formation of ion-conductive channels which we have directly observed in planar lipid bilayers. The toxin also produces vesicle aggregation, as indicated by an increase of the turbidity. Aggregation and permeabilization have completely different time course and extent upon toxin dose and lipid composition, thus suggesting that they are two independent events. Both time constants decrease by lowering the pH of the bulk phase or by introducing a negative lipid into the vesicles.

Our results indicate that at least three steps are involved in the interaction of *Pseudomonas* exotoxin A with lipid vesicles. After protonation of one charged group the toxin becomes competent to bind to the surface of the vesicles. Binding is probably initiated by an electrostatic interaction because it is absolutely dependent on the presence of acidic phospholipids. Binding is a prerequisite for the subsequent insertion of the toxin into the lipid bilayer, with a special preference for phosphatidylglycerol-containing membranes, to form ionic channels. At high toxin and vesicle concentrations, bound toxin may also induce aggregation of the vesicles, particularly when phosphatidic acid is present in the lipid mixture.

A quenching of the intrinsic tryptophan fluorescence of the protein, which is induced by lowering the pH of the solution, becomes more drastic in the presence of lipid vesicles. However, this further quenching takes so long that it cannot be a prerequisite to either vesicle permeabilization or aggregation.

Pseudomonas exotoxin A shares many of these properties with other bacterial toxins like diphtheria and tetanus toxin.

INTRODUCTION

Bacterial protein toxins, produced by several organisms, express their toxic activity in different ways such as disruption of the target membrane integrity, inhibition of protein synthesis, and blockade of neurotransmitter release (1–4). Despite this diversity, some common steps like binding of the toxin to the host membrane, insertion, and, in some cases, translocation can be observed. Very often the insertion of a toxin into the membrane phase leads to the formation of transmembrane pores. In the case of many cytolysins, pore formation seems to represent the toxic activity itself (3). But also in the case of toxins with intracellular enzymatic activity, like diphtheria toxin, the channel opening appears to be a necessary step for the expression of the toxic activity (5–11). Another feature common to different toxins is the conformational transition of the proteins induced by acidic pH. In fact, low pH seems to force many toxins to expose hidden hydrophobic domains, which facilitate both the incorporation of the protein into the target membrane and the translocation of the entire protein, or of a section of it, into the cytoplasm (4). Among toxins with intracellular target, particularly important is *Pseudomonas* aeruginosa exotoxin A. This toxin is the major virulence factor produced by *Pseudomonas aeruginosa,* a microorganism responsible for severe infections in immunodepressed hosts (e.g., subjects exposed to burns, surgical operations [12], or affected by cystic fibrosis [13]). *Pseudomonas* exotoxin A is a single polypeptide chain comprising 613 amino acids (14), which have been assigned to three structurally and functionally-distinct domains (15–18). An amino-terminal domain, which binds to the cell surface, a central translocational domain, and a carboxy-terminal domain, which inhibits protein synthesis by intracellularly ADP ribosylating elongation factor 2. Like diphtheria toxin (with which it shares also the intracellular target), *Pseudomonas* exotoxin A was reported to increase the permeability of lipid vesicles (19, 20). Using these model membranes we have been able to elucidate some features of the toxin-lipid interaction.

We found that the events leading to insertion and pore formation by exotoxin A are consistent with a general model originally developed for colicin A (21). According to this model (21) a positively charged section of the toxin interacts with negative charges residing on the host membrane. This electrostatic interaction (facilitated by a conformational transition driven by acidic pH) orients an hydrophobic hairpin structure, which

0006-3495/91/12/1388/13 $2.00

penetrates into the lipid hydrophobic core, where it contributes to form a pore. Transitions from a closed to an open (permeable) configuration may be favored by the aggregation of several toxin molecules and the presence of a suitable transmembrane potential. Ions and even toxin segments may pass through these pores to reach the cytoplasm and the metabolic targets of the host cell. This model applies, with minor modifications, to other toxins, which have been shown to increase membrane permeability in lipid vesicles, and planar lipid bilayers (21).

MATERIALS AND METHODS

Toxin

Pseudomonas exotoxin A was purchased from the Swiss Vaccine Institute (Bern, Switzerland) as a lyophilized powder, dissolved in water and added to the vesicle-containing solution without any further purification. According to the purchaser, the toxin is more than 97% pure by HPLC, and it has a mean lethal dose of 0.3 μg/ml on mice. When tried against human or bovine erythrocytes these samples had absolutely no hemolytic activity, confirming they are not contaminated with any hemolysin.

Preparation of lipid vesicles

Small unilamellar vesicles (SUV)[1] were prepared by pulsed sonication (25 W output delivery with a 50% duty cycle) of a solution containing multilamellar liposomes (as described in references 22 and 23). It was run to equilibrium in a buffer containing 70 mM calcein (Sigma Chemical Co., St. Louis, MO), 50 mM NaCl, and enough NaOH to give pH 7.0. SUV were then eluted through a Sephadex G50 column using a buffer (external A) containing 160 mM NaCl, 5 mM EDTA, 10 mM Hepes, adjusted to pH 7.0 by NaOH. All of the external fluorophore was removed by this procedure and SUV (whose average molecular weight is ~10 million) eluted in the void volume to a final lipid concentration of ~1–2 mg/ml.

Lipids used were egg phosphatidylcholine (PC) (P. L. Bio-Chemicals, Milwaukee, WI), phosphatidic acid (PA), phosphatidylserine (PS), phosphatidylglycerol (PG) and phosphatidylinositol (PI) from Avanti Polar Lipids, Pelham, AL), and cholesterol (Fluka, Buchs, Switzerland). These lipids were always more than 99% pure giving a single spot by TLC. The starting lipid concentration was always 6 mg/ml, but different compositions were used as specified in the text. All binary mixtures were on a 1:1 molar basis.

Marker release experiments

Aliquots of SUV, prepared as described above, were introduced into a semimicro quartz cuvette (optical length 1 cm) containing 1 ml of external buffer A at the pH indicated in the text. The cuvette was continuously stirred and was thermostatted at 23°C by an external circulator. The temperature of the cell was checked with a digital thermometer (model 871 by Keithley, Cleveland, OH). Fluorescence (expressed in mV) was measured with a Jasco FP550 spectrofluorimeter (Jasco, Tokyo) equipped with a thermostattable 4-cell sample turret, using a photomultiplyer supply voltage of 440 V and a unitary gain setting of the instrument.

For the calcein experiments, excitation wavelength was set at 494 nm (slit width 5 nm) and emission at 520 nm (slit width 10 nm). Calcein release from the interior of the vesicles was detected as an increase of the fluorescence when the dye became diluted into the external medium and self quenching (which occurs at calcein concentrations larger than 1 μM) was relieved (22). 100% release was determined by addition of 0.8 mM Triton X-100 to the cuvette. Spontaneous release of calcein had a half-time of hours under the most unfavorable conditions (SUV comprised of pure PC), and could be neglected.

Light scattering

Light scattering was measured with the same spectrofluorimeter using both excitation and emission at 530 nm. Intense stirring produced some noise on the trace but was necessary to obtain consistent results and was used throughout. The contribution of calcein fluorescence to the recorded signal was negligible under these conditions.

Tryptophan fluorescence

Intrinsic tryptophan fluorescence was excited at 280 nm and the emission was either scanned from 300 to 400 nm or measured near the maximum at 330 nm.

Planar lipid bilayer experiments

Planar bilayers were formed by apposition of two monolayers (as described in reference 24. The monolayers were obtained spreading at the water–air interface 60 μl of a PC:PS (1:1) mixture (Avanti Polar Lipids) dissolved in *n*-hexane (2 mg/ml). The records were obtained using a List EPC7 amplifier (List Electronic, Darmstadt, West Germany) in the voltage clamp mode. The voltage of the PextoxA-free compartment was defined as the reference voltage. Membrane current was recorded with a commercial VHS video cassette recorder equipped with a digital audioprocessor (Sony PCM 601 ESD) modified according to Bezanilla (25). The recordings were filtered through a KEMO VBF8 filter (Kemo, Beckenham, UK) and digitized off line using an Instrutech A/D/A board (Instrutech, Elmont, NY) interfaced to a 4 Mega ST Atari personal computer.

Binding experiments

Toxin binding to lipid vesicles was assayed following a procedure we have already described for other toxins (26). Briefly, 100 μl of vesicles were adjusted to the desired pH by addition of HCl and then mixed with 20 μg of toxin and incubated 30 min at 25°C. Unbound toxin was removed by two-fold filtration over Amicon filters YMT100, with cut off at molecular weight 100 kD (Amicon, Danver, MA), mounted in an Amicon MPS-1 micropartition system (5 min centrifugation at 340 *g*). The volume of the final semi-dry retentate was adjusted to 70 μl with buffer A. The filtrate was collected and concentrated to the same volume by ~30 min centrifugation at 4,000 *g* in Centricon 10 microconcentrators (equipped with Amicon PM10 membranes, with cut off 10 kD).

Polyacrylamide gel electrophoresis

SDS gel electrophoresis was performed according to Laemmli (27) on precast polyacrylamide minigels (with a polyacrylamide density gradient ranging from either 10 to 15% or 8 to 25%) purchased by Pharmacia, Uppsala, Sweden. A semi-automatic unit, PhastSystem by

[1]Abbreviations used in this paper: calcein, fluorescein complexon; PA, phosphatidic acid; PG, phosphatidylglycerol; PC, phosphatidylcholine; PS, phosphatidylserine; PI, phosphatidylinositol; SUV, small unilamellar vesicles; and PextoxA, *Pseudomonas* exotoxin A.

Pharmacia, was employed. Proteins were separated at 10°C in a buffer containing 0.5% SDS. Before running, all protein samples were made 0.8% in SDS; when the toxin had been incubated with lipid vesicles 1 mM Triton X-100 was also included to better solubilize the lipid bilayer. Gels were stained with Coomassie brilliant blue or with silver stain and the amount of protein was quantitated by bidimensional densitometry using a PhastImage densitometer (Pharmacia) with a band-pass filter at 613 nm, for Coomassie-stained gels, or at 546 nm, for silver-stained gels. The relative toxin concentration is given as the optical volume of the corresponding band measured in mOD mm^2.

RESULTS

Pseudomonas exotoxin A permeabilizes lipid vesicles

Addition of *Pseudomonas* exotoxin A to a cuvette containing small unilamellar vesicles loaded with calcein (at a self quenching concentration) promotes the release of the dye. As a consequence the total fluorescence of the sample increases, Fig. 1. The time course of the kinetics of the interaction of the toxin with the vesicles and the dependence on different parameters like the concentration and lipid composition of the vesicles, and the dose of the toxin, can thus be determined.

An adequate fit of the time course of the interaction was always obtained using just a single time constant (an example is shown in Fig. 1). In a few cases the sum of two exponential components with different time constants could give a better fit. However, even in those cases the amplitude of the slower component exceeded that of the faster component by at least a factor of 5, implying first that this component alone described more than 80% of the kinetic process, and second that it coincided (within experimental error) with the first-order time constant. For the sake of simplicity (and because the fast component proved to be slightly dependent on the mixing protocol) in the following, we will only report data obtained by the fit with a single time constant.

Permeabilization depends on the pH and the surface charge of the lipid

Permeabilization of lipid vesicles induced by PextoxA requires low pH. The detailed effects of pH on the rate constant (the inverse of the time constant) and on the

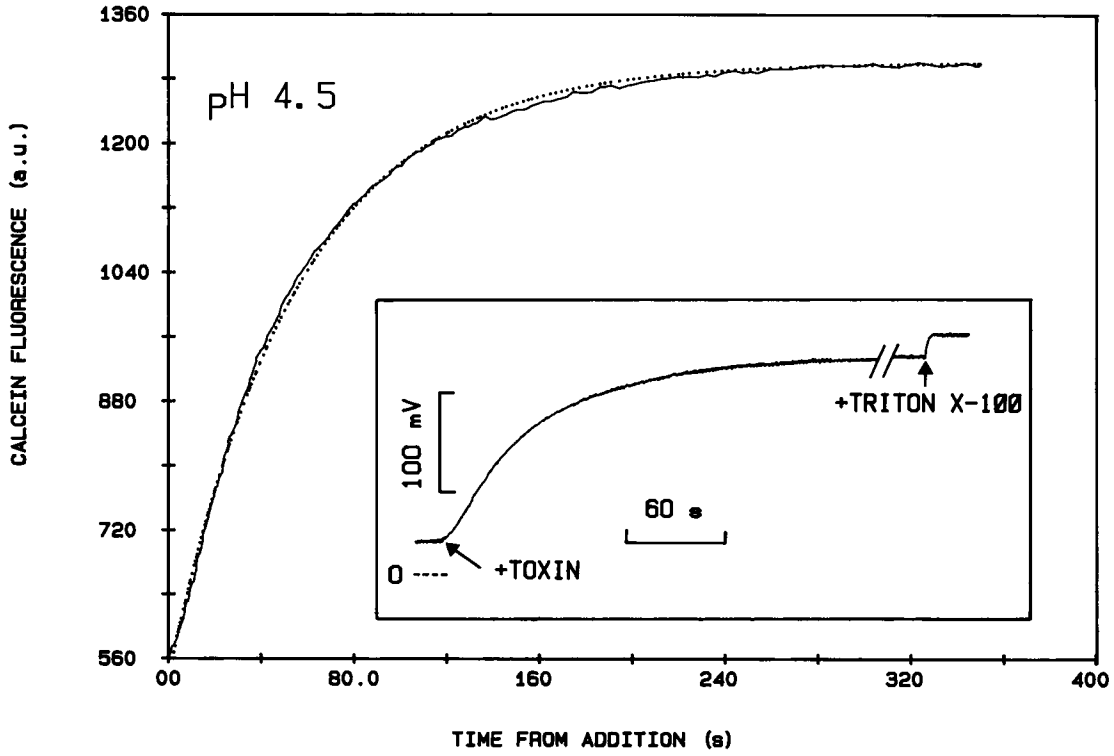

FIGURE 1 PexToxA (40 μg/ml) induces permeabilization of PC/PS vesicles at pH 4.5 as revealed by the increase of fluorescence of calcein when this is released into the external solution. The original trace is shown in the inset. An arrow indicates the addition of exotoxin to the bath solution. 100% release was obtained by the addition of 0.5 mM Triton X-100 as indicated. Final lipid concentration was ~5 μg/ml. The solid trace in the figure are the experimental data after digitization (expressed in arbitrary units). They can be fitted by a kinetics described by a single exponential decay with time constant τ (*dotted line*). For the experiment reported in this figure τ = 56 s.

percentage of calcein release are shown in Fig. 2, *A* and *B*, respectively, for different compositions of the lipid vesicles. It can be observed that calcein release becomes relevant only at a pH lower than 6 and with vesicles containing negatively charged lipids. Within pH 4.0 and 5.5, a pH shift of one unit produces a rate constant change of approximately a factor of ten. This direct proportionality suggests that binding of protons to the toxin is necessary to make it competent to interact with the lipid. The apparent pK of the permeabilization does not seem to depend much on the surface potential because PS and PC/PS vesicles behave similarly, and so do PC/PG and PC/PI. The apparent pK of the protonable group of the toxin is 4.4 ± 0.2. Noteworthy, this value corresponds to the pH at which *Pseudomonas* exotoxin A experiences a conformational change exposing a hydrophobic domain (28) and acquiring the ability to bind Triton X-114 (29). However, in neutral lipids PextoxA remains virtually ineffective even at low pH (the percentage of release is at most 10% in PC vesicles, Fig. 2 *B*), indicating that low pH is necessary but not sufficient for permeabilization. Calcein release in PC vesicles is so small that the evaluation of the rate constant is unreliable and therefore not reported in Fig. 2 *A*.

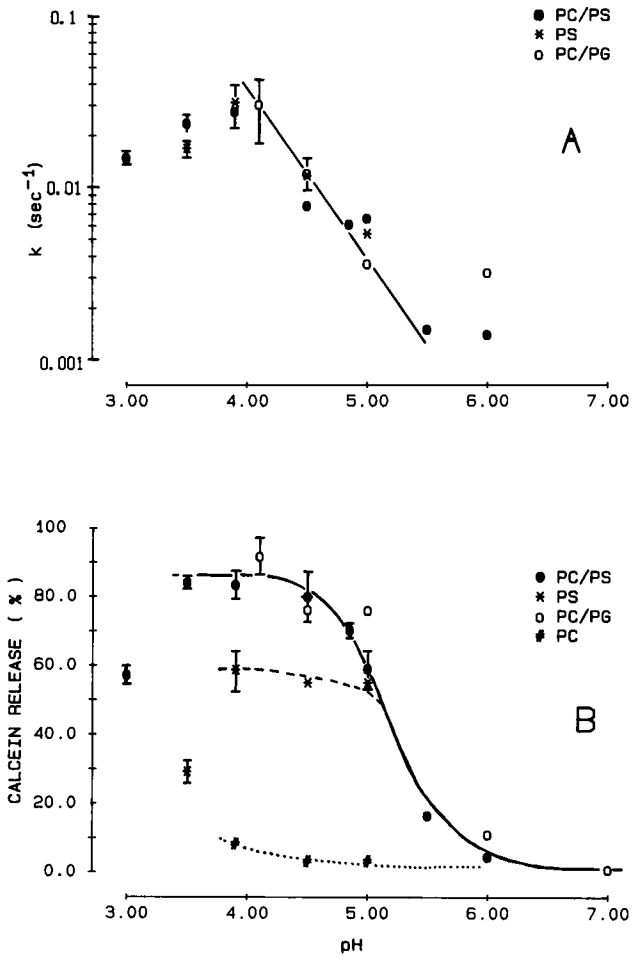

FIGURE 2 pH dependence of the kinetics of interaction of PexToxA with phospholipid vesicles of different composition. (*A*) Rate constants, *k*, describing calcein release are plotted versus the pH of the bath solution (the solid line drawn is for a tenfold change for each pH unit). Rate constants larger than 0.003 s^{-1} are observed only with vesicles containing acidic phospholipids at a pH lower than 6. (*B*) Percentage of release for the same experiments. It can be observed that release is almost undetectable in neutral lipids (pure PC) and it is larger when PG is used instead of PS (the lines through the experimental points do not have a theoretical meaning).

The decrease of activity, which can be observed at pH values lower than 4.0, is possibly due to a partial inactivation of the toxin either because of an irreversible conformational change (28, 36, 41) or because of a self aggregation (47) as observed for diphtheria toxin (42).

Experimental conditions: PextoxA concentration was 40 μg/ml except for PC/PG vesicles for which it was 10 μg/ml; Phospholipid concentration was 5 μg/ml throughout.

Exotoxin A forms ionic channels in planar lipid bilayers

Vesicle permeabilization induced by PextoxA may result from the formation of toxin channels into lipid bilayers, like it has been shown for diphtheria and tetanus toxins. To check this possibility we tested the interaction of PexToxA with planar lipid bilayers. We observed square shaped current transitions typical of single ionic channel mechanisms, which are occasionally clustered in current bursts. A broad distribution of channel amplitude was observed, thus suggesting that ionic channels may result from the formation of heterogeneous toxin aggregates. In Fig. 3 *A* it is reported a long lasting burst observed in a PC:PS (1:1) membrane, which presents a current amplitude of ~3.0 pA (applied voltage +100 mV). A mean conductance of 31 pS was obtained analyzing 251 events by a 50% threshold criteria (Fig. 3 *B*). The bell-shaped open-time distribution observed is representative of a single time constant, which was well fit by a mean open time of 1.1 ms.

Exotoxin A induces also aggregation of lipid vesicles as an independent process

Because diphtheria toxin (which shares structural and functional features with PextoxA [29, 30]) has been shown to induce massive aggregation of lipid vesicles (31, 32), we investigated this aspect also with PextoxA. We found that, under appropriate conditions, PextoxA induces vesicle aggregation as evidenced by an increase

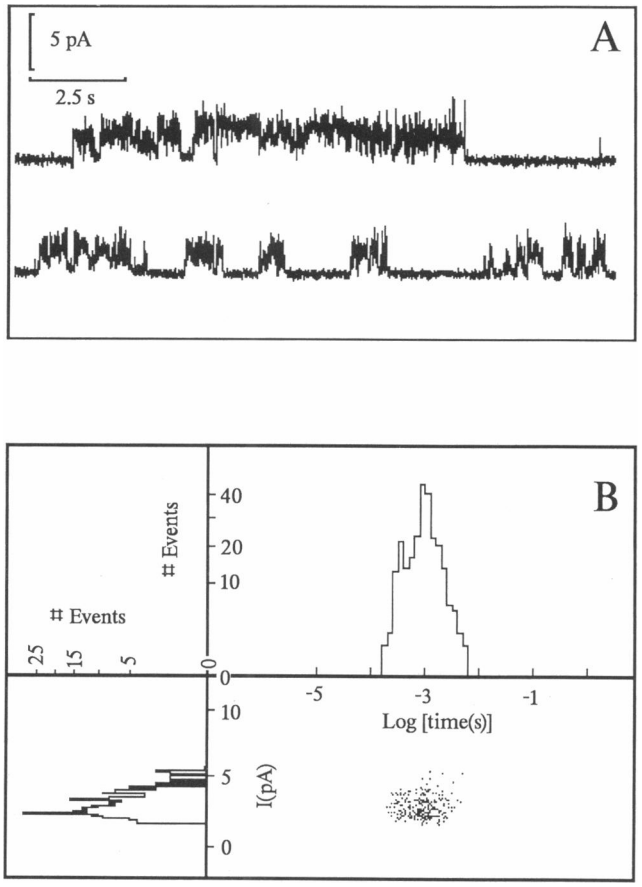

FIGURE 3 (*A*) A PextoxA current burst recorded in PC:PS membrane in the presence of 70 μg/ml toxin is shown. This burst is formed by a series of consecutive openings with a conductance of ≈30 pS, typical of PextoxA. Channels of smaller and higher amplitudes were occasionally observed. Moreover, open-closed transitions with PextoxA usually occur as few consecutive events followed by long lasting closures. In *B*, the result of the analysis performed on such events according to reference 44 is reported. In the third quadrant, the histogram describing the number of events as a function of the current amplitude is shown using a square root ordinate display, it gives a mean current amplitude of 3.1 pA. In the first quadrant, a duration histogram is plotted showing a square root ordinate display of the number of events versus the decimal logarithm of their open time. The single peak is representative of the existence of a single open time evaluated in 1.1 ms. In the second quadrant, the scatter plot of the events is shown. Analysis was performed on 251 events and gave a mean open probability of 4×10^{-3}. The aqueous solution was KCl, 100 mM; Mes, 10 mM buffered at pH 5.5 with KOH. The filter was set at 100 Hz for signals reported in *A* and at 1 kHz to analyze data reported in *B*. Applied voltage was +100 mV.

of the turbidity after toxin addition (Fig. 4). Therefore, it was important at this point to assess whether the permeabilization of the vesicles was a consequence of their aggregation or not. This possibility was investigated by determining simultaneously the kinetics of release and aggregation at different toxin and lipid concentrations and with different lipid compositions.

The rate constant and the percentage of calcein release versus the dose of toxin are shown in Fig. 5, *A* and *B*, respectively, for two different compositions of the lipid vesicles. The extent of release first increases and then saturates at ~95% for PC/PG vesicles and at 80% for PC/PS vesicles. For PC/PG vesicles the rate constant increases almost linearly with the concentration of the toxin, while PC/PS vesicles show a linear trend in a narrow range of toxin concentration. Moreover, at any toxin concentration PC/PG vesicles are more sensitive to PextoxA than PC/PS vesicles, since the calcein release is more extensive and faster. Interestingly, when we consider the light scattering increase due to vesicle aggregation (Fig. 5 *C*), it appears that this effect only becomes relevant at higher toxin concentrations, as compared with permeabilization. As an example, in PC/PG vesicles at a toxin concentration of 1 μg/ml the extent of release is already 90% of the maximum value, whereas the increase in turbidity is negligible (only 3.3% of the maximum effect observed).

When the dependence of permeabilization and aggregation on the vesicle concentration was investigated (with PC/PS vesicles at toxin concentration of 40 μg/ml), again we found that these two effects behave differently (Fig. 6). In fact, the extent of release is nearly independent of the vesicle concentration (Fig. 6 *B*), whereas the increase in turbidity strongly depends on it and is insignificant at the lowest vesicle concentration used. Moreover, the two rate constants show an opposite behavior (Fig. 6 *A*): the rate of permeabilization slightly decreases, increasing the vesicle concentration, whereas the rate of aggregation definitely increases. This last effect was not unexpected since aggregation (relying on the encounter of two vesicles) should indeed be favored by higher vesicle concentrations. On the contrary, permeabilization is under pseudo-first order conditions in these experiments (because the toxin to vesicle molar ratio is always very large, i.e., 30:1 under the most unfavorable conditions) and hence it is expected to be independent of vesicle concentration (23).

Finally, the time course and extent of vesicle permeabilization and aggregation, using vesicles of different lipid composition, are compared in Fig. 7. Again we found differences between the increase of light scattering and the calcein release. Particularly, the presence of PA strongly enhances the first process but does not induce any release. On the contrary, PI and PG, which strongly enhance the release, do not stimulate large aggregation. However, vesicles composed of pure PC were refractory to both of the mentioned effects.

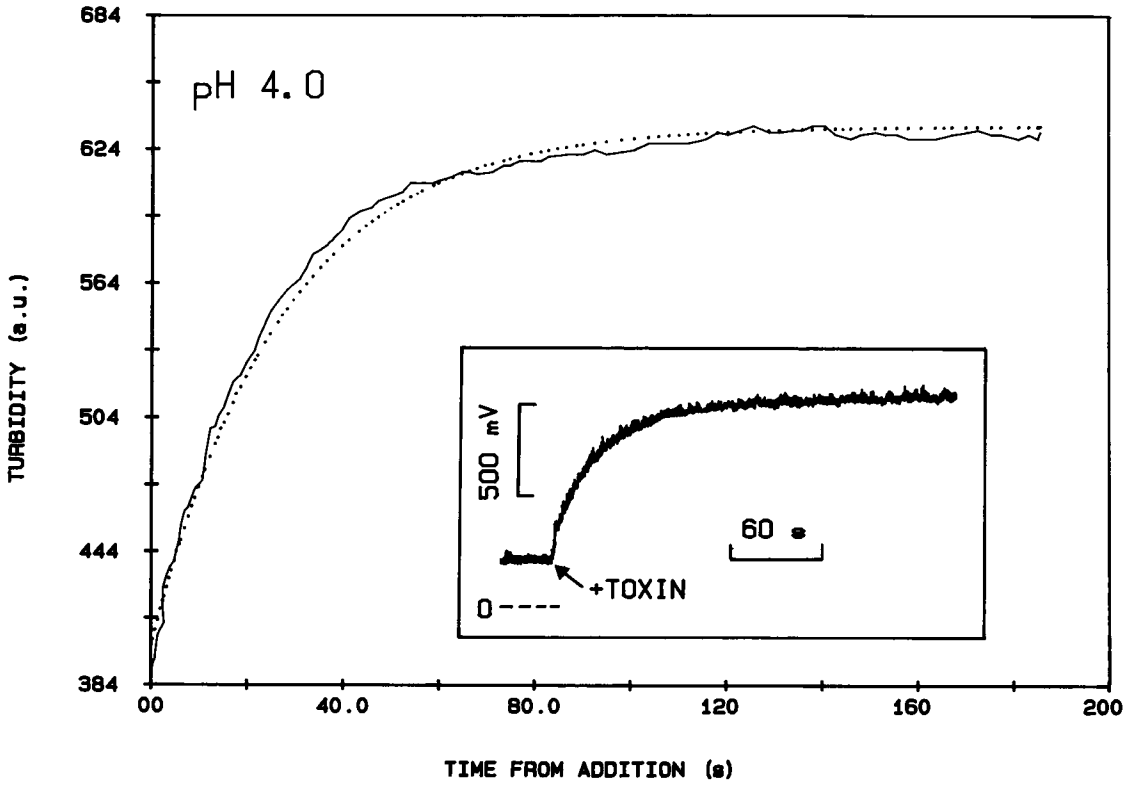

FIGURE 4 PexToxA induced aggregation of PC/PS vesicles at pH 4.0 as revealed by the increase of the scattered light at 530 nm. The original trace is shown in the inset. The arrow indicates the addition of 40 μg/ml of toxin to the bath solution. Final lipid concentration was ~5 μg/ml. As in the case of calcein release (Fig. 1), the digitized experimental data (*solid trace* in the figure) can be fitted by a kinetics described by a single exponential decay (*dotted line*). For the experiment reported in this figure $\tau = 40$ s.

Correlation between binding of toxin to lipid vesicles and their permeabilization

Lipid vesicles incubated with PextoxA can be separated from unreacted toxin by centrifugal filtration over planar filters of large molecular weight cut-off (100 kD). It is then possible to quantitate by SDS-PAGE the amount of toxin bound (i.e., retained over the filters) and the unbound fraction (i.e., present in the filtrate), Fig. 8. This demonstrates that the interaction of the toxin with the target vesicles is stable. When calcein-loaded vesicles are used for these binding experiments it is further possible to measure the calcein fluorescence both in the filtrate and in the retentate either before or after addition of a detergent (Triton-X100). In this way we can measure simultaneously both toxin binding and extent of vesicle permeabilization under different experimental conditions, Figs. 9 and 10.

When the effect of pH on the action of PextoxA on PC/PS vesicles is studied (Fig. 9) it becomes clear that binding and permeabilization are directly correlated. In fact, at pH values lower than 5 most of the toxin is bound and all of the calcein is released, while at pH larger than 5 the opposite is true, i.e., most of the toxin is unbound and most of the calcein is retained inside the vesicles. At pH 5 the situation is intermediate.

When the effect of the lipid composition of the vesicles is considered we have a similar situation, but with one noticeable exception. In fact, if on one hand with PC and PC/cholesterol vesicles we observed little binding and little permeabilization, whereas with PC/PS, PC/PI, and PC/PG we found good binding and almost complete calcein release; on the other hand, with PC/PA vesicles most of the calcein is retained inside the vesicles even though the toxin is bound to a good deal. This is consistent with the results in Fig. 7, where it was shown that PC/PA vesicles, though not permeabilized, are effectively aggregated by PextoxA, indicating that some kind of binding was taking place.

DISCUSSION

The interaction of a protein with lipid vesicles can be treated as a particular case of the more general interac-

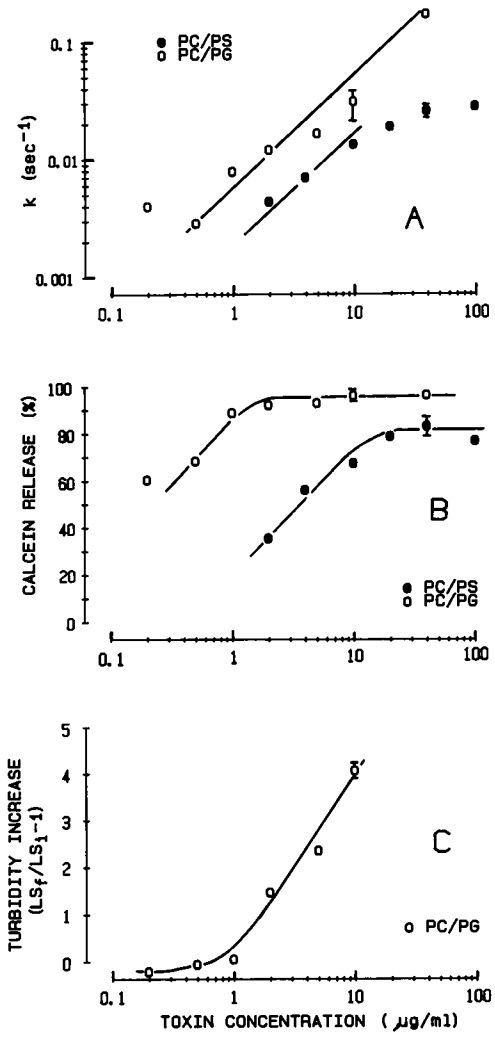

FIGURE 5 Kinetics of calcein release and vesicle aggregation versus PexToxA concentration. (*A*) Rate constants, *k*, describing the permeabilization of vesicles with two different phospholipid compositions are reported in a bilogarithmic scale as a function of exotoxin concentration in solution. Despite the fact that experiments with PC/PG were performed at a slightly higher pH (4.1) with respect to PC/PS (pH 3.9), a larger rate constant is measured in the first case at any toxin concentration (*solid lines* drawn have a slope of one). (*B*) Percentage of release, plotted in a half-logarithmic scale, versus PexToxA concentration. In consistence with *A*, PC/PG vesicles show a larger degree of release as compared with PC/PS vesicles and a saturation at ~ 95% of the maximum release possible for toxin concentrations ≥1 μg/ml. Release in PC/PS vesicles was in the order of 80% of maximum at a toxin concentration ≥20 μg/ml (*solid lines* were drawn by eye). (*C*) A quantitative indication of vesicle aggregation is obtained from the ratio $(LS_f/LS_i - 1)$, where LS_f is the final light scattering measured in the presence of toxin, and LS_i is the initial light scattering measured before PexToxA addition. It can be observed that PC/PG vesicles start to aggregate only at a PexToxA concentration ≥1 μg/ml, whereby calcein release is already saturated (*solid line* drawn by eye). Phospholipid concentration was 5 μg/ml throughout.

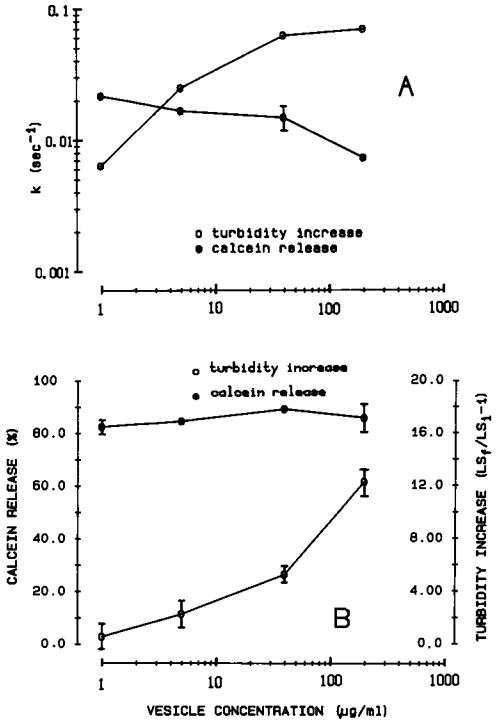

FIGURE 6 Comparison of calcein release and vesicle aggregation kinetics as a function of lipid concentration. (*A*) the rate constant, *k*, of calcein release measured in PC/PS vesicles at pH 4 and in the presence of 40 μg/ml of PexToxA slightly decreases with vesicle concentration (in the range 1–200 μg/ml of lipid), while (in the same conditions) the rate constant describing vesicle aggregation markedly increases and seems to saturate only at lipid concentrations above 40 μg/ml. (*B*) Vesicle concentration does not affect the percentage of calcein release (units on the left *y* axis), whereas the variation of light scattering, normalized with respect to the initial value as in Fig. 5 (units on the right *y* axis), shows that aggregation increases dramatically with vesicle concentration.

tion of a macromolecule with a large aggregate of targets (33, 34). Such interaction in general evolves in several steps; for the case of PextoxA our results indicate the following scheme as the minimal one:

$$T_f + V \underset{k_{-d}}{\overset{k_d}{\rightleftharpoons}} T_{enc} \underset{k_{-a}}{\overset{k_a}{\rightleftharpoons}} T_{ads} \underset{k_{-i}}{\overset{k_i}{\rightleftharpoons}} T_{ins} \qquad (1)$$
$$+V\, k_{agg} \downuparrows k_{-agg}$$
$$T_{agg}.$$

In this scheme T_f and V represent the free toxin and the vesicles in solution, T_{enc} is an "encounter" state populated by toxin molecules which have approached the surface of the vesicles, T_{ads} represents toxin firmly adsorbed onto the vesicles, T_{ins} represents toxin inserted into the bilayer, and T_{agg} toxin which participates in the aggregation of the vesicles. The T_{enc} state is a purely

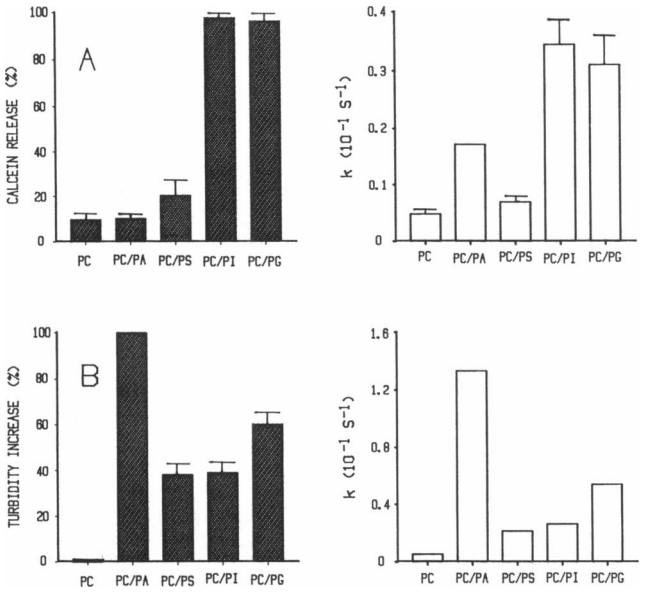

FIGURE 7 Effect of lipid composition on the interaction of PextoxA with lipid vesicles. Comparison of (*A*) calcein release and (*B*) vesicle aggregation is represented by the percentage of the effect (*left*) and the corresponding rate constant, *k*, (*right*) for five different phospholipid compositions. All experiments were performed at pH = 4.1, in the presence of 10 μg/ml PexToxA and 5 μg/ml lipid. PC/PI and PC/PG evidently are the two lipid compositions favoring the permeability increase mediated by the toxin (*A*). However, these two mixtures give rise to little vesicle aggregation as compared with PC/PA vesicles (*B*). From the other hand, PC/PA vesicles, which are affected by a relevant aggregation process (*B*), are not permeabilized by the toxin (*A*).

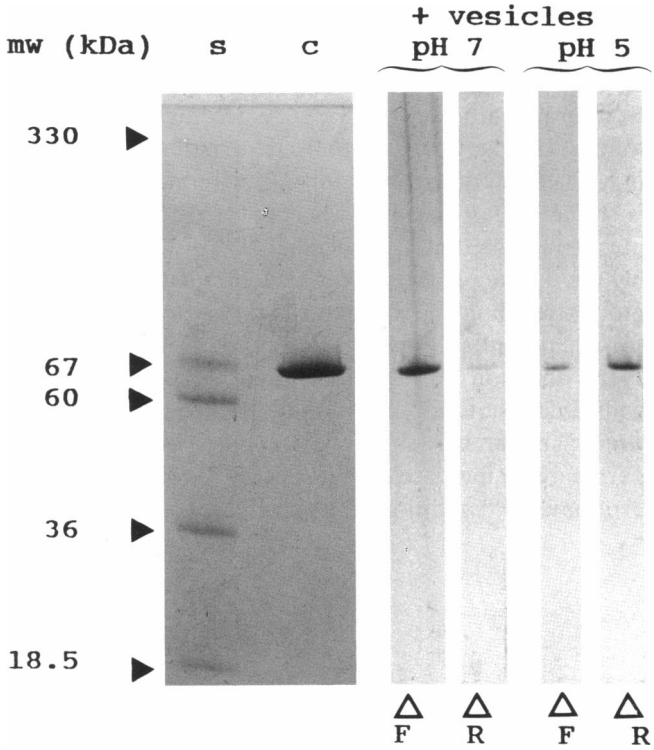

FIGURE 8 PextoxA binding to lipid vesicles. In SDS-PAGE, PextoxA (lane *c*) runs as a single band of molecular weight 67 kD (as compared with molecular weight standards in lane *s*).

When unilamellar vesicles (lipid concentration 670 μg/ml) are incubated with PextoxA (167 μg/ml), the bound toxin can be separated from the unreacted toxin by filtration over large molecular weight cut-off filters (100 kD) which allow free toxin but not vesicles to pass through. The retentate and the filtrate can then be electrophoresed separately (lanes indicated by letters *R* and *F*, respectively). Using PC/PS vesicles, it appears that at pH 7 most of the toxin is unbound (i.e., it is present only in the filtrate), whereas at pH 5 a large fraction of it is bound (i.e., it is retained over the filter). It is further possible to quantitate the toxin bound and the toxin unbound by reading the optical density of the bands separated by SDS-PAGE. Total protein content is proportional to the volume of the band (optical density × area) and is measured in mOD · mm²; such values are used in Figs. 9 and 10.

Other experimental conditions: lanes *s* and *c* were stained with Coomassie blue while the others were silver-stained; a polyacrylamide gradient from 10 to 15% was used.

geometrical state (33) in continuous exchange with free toxin, T_f, by diffusion in the water solution with rate constants k_d and k_{-d} (forward and backward diffusion, respectively). We can calculate k_d and k_{-d} using their usual expressions (which can be found in references 23 and 33). First we estimate the toxin diffusion coefficient D from its molecular weight (35) getting $D = 0.8\ 10^{-6}$ $cm^2\ s^{-1}$. From this (33) we obtain $k_{-d} = 0.84\ 10^6\ s^{-1}$ (indicating that the average lifetime of T_{enc} is 1.2 μs) and $k_d = 1.1\ 10^6\ M^{-1}\ s^{-1}$ (where the molar lipid concentration was used). Comparing the calculated k_d with the observed permeabilization rate for PC/PG vesicles $k_{obs} = 0.25\ 10^6\ M^{-1}\ s^{-1}$ (obtained from Fig. 4), we conclude that even in the case of the most sensitive vesicles the interaction is slower than the diffusion limit implying that it is rate limited by the successive steps.

T_{enc} may evolve to T_{ads}, i.e., toxin adsorbed onto the vesicles, with rate constants k_a and k_{-a} (forward and backward rate, respectively). The state T_{ads} is introduced to account for our binding results (Figs. 8–10). In fact we have observed the existence of a state in which the toxin is bound to the lipid vesicles, firmly enough to be separated from unbound toxin, but still unable to permeabilize the vesicles (e.g., lipid composition PC/PA).

Our data indicate that both low pH and negatively charged lipids are required for the occurrence of T_{ads}, suggesting that this state is the result of an electrostatic interaction of toxin molecules with acidic phospholipids. In agreement with this idea, it has been found that the presence of positively charged lipids in the vesicles prevents any incorporation of the toxin into the bilayer

(36). In analogy with diphtheria toxin, we believe that the role of low pH is to induce a conformational change of the toxin leading to a relaxed structure more suitable to interact with a lipid phase. Accordingly, we assume that k_a is not zero only for those toxin molecules, that are in a protonated lipophilic form. Furthermore, since T_{ads} is stable even when T_f is removed (see Figs. 8–10), we must conclude that k_{-a} is negligible. This is most probably due to the electrostatic interaction between positive groups residing on the toxin and the vesicle negative surface potential.

By diffusion through the lipid bilayer (with rate constants k_i and k_{-i}) eventually T_{ads} may evolve to T_{ins} which, in our model, is the form responsible for the permeability increase of the vesicles. Under most of our experimental conditions the parallel reaction leading to T_{agg} is not operating. Accordingly, pore formation is controlled only by the reactions connecting T_f to T_{ins}.

Because of the small dimensions of our vesicles the formation of one toxin channel, with a conductance as measured in planar bilayers, would dissipate the gradient of any permeant molecule within less than one second (37), i.e., much faster than our experimental resolution. This ensures that the rate limiting event we observe is the formation of channels into the vesicles and not the exit of calcein from each single vesicle.

The possibility that the permeabilizing effect observed is actually the result of a fusogenic action of *Pseudomonas* exotoxin A on lipid vesicles as a consequence of their aggregation (because fusion of SUV often promotes a release of entrapped markers as a secondary effect) can be ruled out. In fact, we have found that under some circumstances aggregation precedes calcein release but in most cases permeabilization occurs long before any aggregation (Fig. 4). Furthermore, we have found experimental conditions like low toxin concentration (i.e., $T_f \leq 1$ μg/ml with 5 μg/ml PC/PG vesicles pH 4.1; Fig. 4), high pH (pH $\geq$ 5 with T_f = 10 μg/ml and 5 μg/ml PC/PG vesicles; data not shown), and low vesicle concentration ([lipid] $\leq$1 μg/ml with PC/PS vesicles, pH 4.0 and T_f = 40 μg/ml; Fig. 5), under which strong release (always more than 60%) and virtually no aggregation is observed. Conversely, with 5 μg/ml PC/PA vesicles at pH 4.1 and T_f = 10 μg/ml massive aggregation occurs with only ~10% permeabilization (Fig. 7). A similar

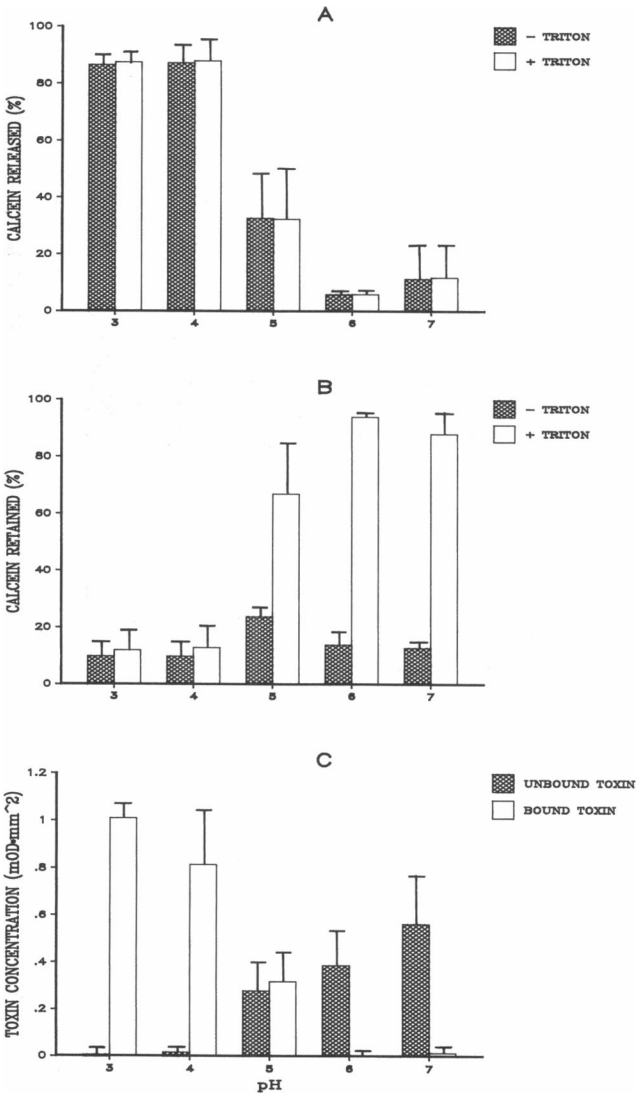

FIGURE 9 Calcein fluorescence and protein content of the two phases (filtrate and retentate) obtained from centrifugation on planar filters of PC/PS vesicles (670 μg/ml) treated with PexToxA (170 μg/ml) at different pH. (*A*) The fluorescence due to calcein present in the filtrate, before (*filled bars*) and after (*empty bars*) addition of Triton X-100, is reported. Filled and empty bars are almost identical, confirming that the calcein present in the filtrate is not associated with lipid vesicles. An acidic pH clearly increases the percentage of free calcein present in the filtrate. (*B*) Fluorescence of calcein present in the retentate before (*filled bars*) and after (*empty bars*) the addition of detergent. Only at high pH is calcein retained. The increase of fluorescence after addition of Triton X-100 clearly shows that the retained calcein is entrapped into the vesicles since its fluorescence was quenched before the addition of the detergent. (*C*) Optical density measurements (on SDS gels prepared as in Fig. 8), show that toxin bound (i.e., recovered in the vesicle phase; *empty bars*) has a pH dependence closely parallel to that of released calcein (*A*), whereas toxin unbound (*filled bars*) parallels retained calcein (*B*). Other conditions as in Fig. 8. A systematically slightly higher density of the bands corresponding to toxin bound to lipid vesicles (here and in Fig. 10) may be due to a better staining of this hydrophobic form of the protein as compared with the water soluble form, but in no case was it so relevant to impair the validity of the conclusions on protein distribution.

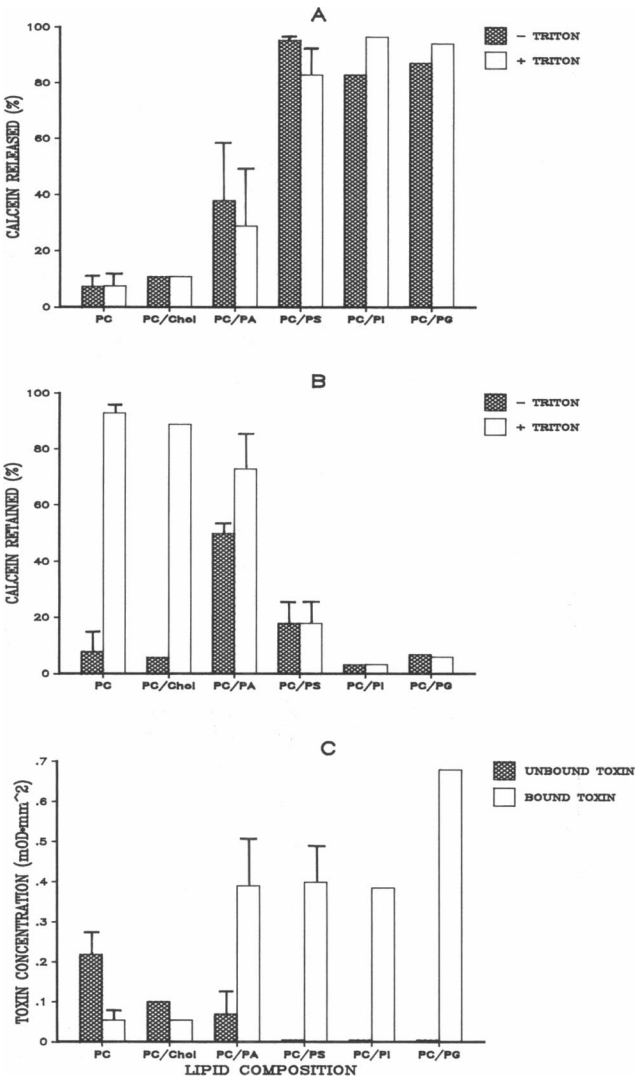

FIGURE 10 The fluorescence of calcein in the filtrate (*A*), in the retentate (*B*), and the optical density quantitating toxin binding to the vesicles (*C*) were measured as described in Figs. 8 and 9, as a function of the lipid composition of the vesicles at pH 4.0. Also, in this case filled and empty bars in *A* and *B* represent the fluorescence measured before and after treatment with Triton X100, respectively. The three panels show consistent trends, i.e., lipid mixtures that produce a negligible permeability increase (*two left couple of bars* of *A*) present still most of the calcein entrapped inside (*B*) and exhibit little toxin binding to the lipid phase (*C*). On the contrary, lipid mixtures presenting the higher permeabilization have the opposite behavior. PC/PA mixture is an exception because, to a very limited permeabilization, corresponds a lipid binding comparable to that of PC/PS and PC/PI.

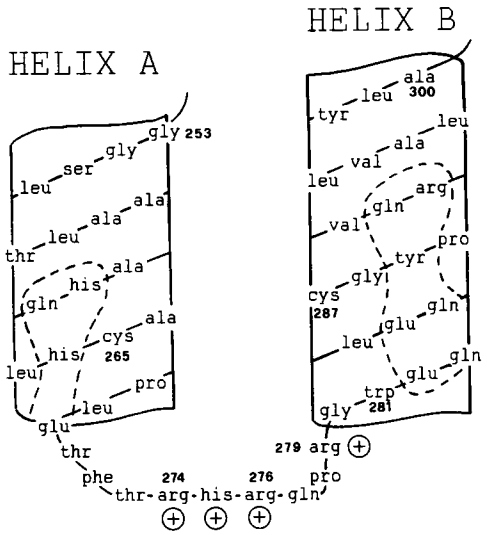

FIGURE 11 Putative region of PextoxA responsible for its interaction with lipid membranes. This region, encompassing residues 253 to 300, includes the first two α-helices of domain II, which are termed *A* and *B*, respectively (15). Helix A is largely apolar whereas helix B is more amphiphilic. Polar residues, according to Kyte and Doolittle (45), have been included in a dashed contor. The two alpha helices are linked by a disulfide bond between cys_{265} and cys_{287}. The connecting region (random coil [15]) contains a cluster of four positive charges (three arg and one his), which are proposed to trigger an electrostatic interaction with negatively charged phospholipids. The position of the sole trp residue is also given.

independence between the aggregating and the permeabilizing activity has been observed with diphtheria toxin (32, 38).

We assume that the aggregation reaction occurs from T_{ads} in parallel to the formation of T_{ins}. We may write:

$$T_{ads} + V \underset{k_{-agg}}{\overset{k_{agg}}{\rightleftharpoons}} T_{agg}, \qquad (2)$$

which represents the coordination of a second vesicle by the toxin adsorbed on one vesicle. This reaction, which leads to effective aggregation of two vesicles, is itself most probably due to an electrostatic attraction between adsorbed toxin and the surface of a second vesicle; in fact, vesicles containing PA (which, owing to the small volume of the polar head, are expected to have a higher surface potential) are the most effectively aggregated by PextoxA (Fig. 7). A similar mechanism has been proposed for diphtheria toxin (32, 38). Based on this scheme the aggregation rate is expected to depend on the vesicle concentration, which appears explicitly in Eq. 2, as we have verified in our experiments (Fig. 6).

Finally, when the lipid-induced quenching of the intrinsic tryptophan fluorescence is considered (see Appendix A) one should notice that its lipid dependence is the same as that of aggregation, thus suggesting that it is also a consequence of the formation of T_{ads}. On the other hand, its rate constant is the smallest observed,

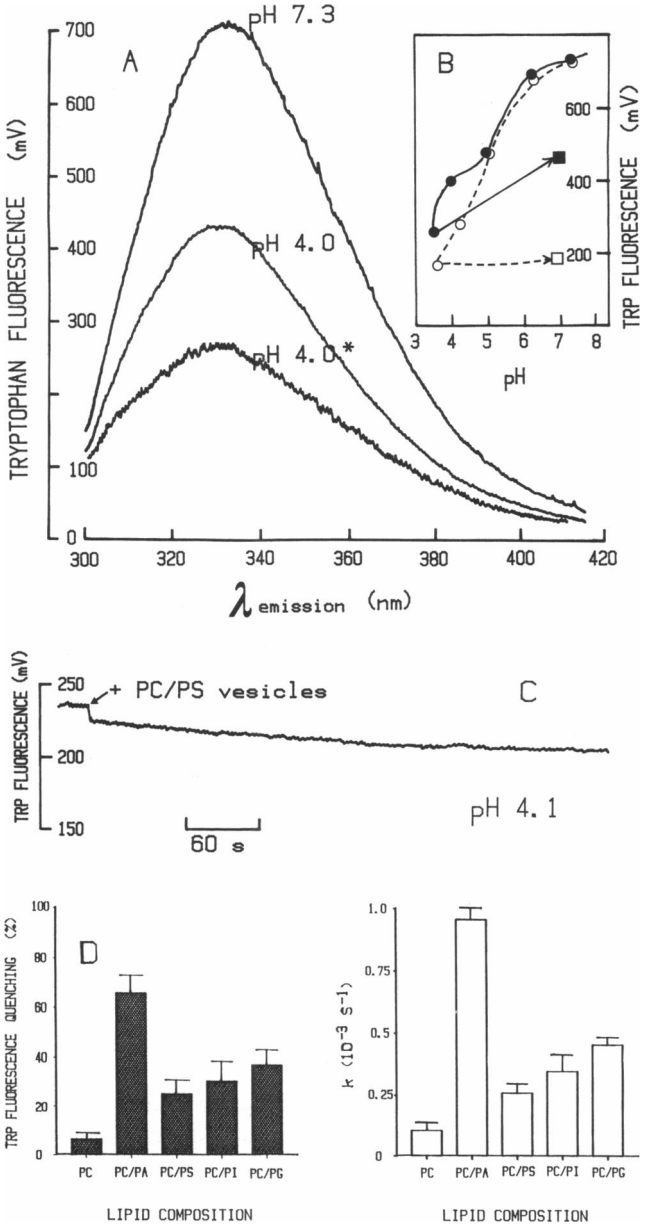

FIGURE 12 Conformational change of PextoxA at low pH. (*A*) Intrinsic triptophan fluorescence of PexToxA at a toxin concentration of 20 μg/ml (excitation wavelength 280 nm), in 160 mM NaCl, 5 mM EDTA, 10 mM Hepes, at pH 4.0 and 7.3. The quenching of fluorescence induced by acid pH possibly represents a conformational transition of the protein. Quenching is enhanced when the pH is lowered in the presence of 50 μg/ml PC/PS vesicles (*lower curve* at pH 4, indicated by an *asterisk*). Fluorescence is measured in mV. (*B*) Maximal tryptophan fluorescence of PexToxA (20 μg/ml) as a function of pH, either in the absence (*filled points, solid line*) or in the presence (*empty points, dashed line*) of 50 μg/ml PC/PS vesicles. The pH of the toxin sample was progressively lowered (*circles*); at the end the reversibility of the quenching was tested by cycling back both the samples to pH 7 (*squares*). Two indications can be obtained: first, the presence of vesicles favors the conformational transition of the toxin occurring at acidic pH; second, the binding of PexToxA to vesicles is almost irreversible. (*C*) Time course of the change in the maximal tryptophan fluorescence of PexToxA (10 μg/ml) at pH 4.1 after addition of 6 μg/ml PC/PS vesicles. Quenching of toxin fluorescence by phospholipid is a very slow process taking several minutes. (*D*) Effect of lipid composition on the toxin conformational change. Experimental conditions as in *C*.

and therefore these lipid-induced conformational transitions of the toxin are not required either for the aggregation or for the permeabilization of the vesicles. It might then reflect a long term rearrangement of the protein (after its adsorption onto the vesicle surface) in a region of the molecule that is not directly involved in the perturbation of the lipid bilayer.

A structural model of the interaction of PextoxA with lipid vesicles

The negative surface potential requirement for the formation of T_{ads} suggests that a stretch of positively charged residues is involved in toxin binding (38, 39). We found one such stretch in domain II, the part of PextoxA molecule known to mediate the interaction with the membrane (16).

This stretch (encompassing residues 274 to 279) includes three arginines and one histidine (Fig. 11), and is located between two alpha helices linked by a disulphide bond between cys_{265} and cys_{287} (15), which are either rather apolar (helix A) or clearly amphiphilic (helix B). In analogy with other channel forming proteins (e.g., colicin A [40]), we propose the following steps of interaction: low pH induces a partial unfolding of the protein with enhanced exposure of trp residues to the polar solvent ([41] but see also Fig. 12) and a less tight packing of helices A and B to the rest of the molecule; this opens the possibility for (*a*) electrostatic binding of the loop containing the arginine cluster to negatively charged lipids (a prerequisite for aggregation), and (*b*) insertion of the two amphiphilic helices into the hydrophobic phase with concomitant translocation of the arginine cluster to the other side of the membrane (a prerequisite for permeabilization).

APPENDIX

Effect of lipid vesicles on the conformational change of *Pseudomonas* exotoxin A induced by low pH

It has been reported (28, 41) that the conformational change of PextoxA at low pH leads to a quenching of its intrinsic tryptophan fluorescence probably related to the exposure of hydrophobic regions.

We were thus prompted to investigate whether lipid vesicles can also induce a further tryptophan fluorescence quenching of PextoxA (Fig. 12 *A*). We found that, indeed, at pH values at which the toxin increases vesicle permeability, its tryptophan fluorescence is further quenched by the interaction with the vesicles (Fig. 12, *A* and *B*). Interestingly, while the quenching induced by acidic pH is very fast (we could confirm that it occurs in less than 1 min, as reported in reference 28), the further quenching induced by lipid is a very slow process that reaches a steady-state only in about half an hour; Fig. 12 *C*. The quenching is accompanied by a red shift of the maximum of emission from 332 to 336 nm, much similar to that observed with diphtheria toxin (42, 43), which indicates that tryptophan residues become more exposed to the solvent. We further observed that while the pH-induced quenching is largely reversible (as reported also in reference 28) the slow lipid-induced additional quenching is almost irreversible (Fig. 12 *B*).

Despite of the similarity in the lipid dependence of vesicle aggregation and toxin conformational change (compare Fig. 12 *D* with Fig. 7 *B*), the two effects are not coincident since the time course of toxin change is about two orders of magnitude slower than that of vesicle aggregation (note the different time scales in Fig. 7 *B* and 12 *D*).

We wish to thank Richard Horn and Cesare Montecucco for a critical reading of the manuscript and Giovanna Belmonte for technical assistance.

The authors have been financially supported by the Italian Consiglio Nazionale delle Ricerche and Ministero di Pubblica Istruzione.

Received for publication 5 October 1990 and in final form 10 July 1991.

REFERENCES

1. Middlebrook, J. L., and R. B. Dorland. 1984. Bacterial toxins: cellular mechanisms of action. *Microbiol. Rev.* 48:199–221.
2. Bernheimer, A. W., and B. Rudy. 1986. Interactions between membranes and cytolytic peptides. *Biochim. Biophys. Acta.* 864:123–141.
3. Bhakdi, S., and J. Tranum-Jensen. 1987. Damage to mammalian cells by proteins that form transmembrane pores. *Rev. Physiol. Biochem. Pharmacol.* 107:147–223.
4. Olsnes, S., and K. Sandvig. 1988. How protein toxins enter and kill cells. *In* Immunotoxins. A. E. Fraenkel, editor. Kluwer Academic Publishing, New York. 39–73.
5. Donovan, J. J., M. I. Simon, R. K. Draper, and M. Montal. 1981. Diphtheria toxin forms transmembrane channels in planar lipid bilayers. *Proc. Natl. Acad. Sci. USA.* 78:172–176.
6. Kagan, B., A. Finkelstein, and M. Colombini. 1981. Diphtheria toxin fragment forms large pores in phospholipid bilayer membranes. *Proc. Natl. Acad. Sci. USA.* 78:4950–4954.
7. Misler, S. 1983. Gating of ion channels made by a diphtheria toxin fragment in phospholipid bilayer membranes. *Proc. Natl. Acad. Sci. USA.* 80:4320–4324.
8. Papini, E., D. Sadonà, R. Rappuoli, and C. Montecucco. 1988. On the membrane translocation of diphtheria toxin: at low pH the toxin induces ion channels on cells. *EMBO J.* 7:3353–3359.
9. Shiver, J. W., and J. J. Donovan. 1987. Interaction of diphtheria toxin with lipid vesicles: determinants of ion channel formation. *Biochim. Biophys. Acta.* 903:48–55.
10. Olsnes, S., J. O. Moskaug, H. Stenmark, and K. Sandvig. 1988. Diphtheria toxin entry: protein translocation in the reverse direction. *Trends Biochem. Sci.* 13:348–351.
11. Sandvig, K., and S. Olsnes. 1988. Diphtheria toxin-induced channels in Vero cells selective for monovalent cations. *J. Biol. Chem.* 263:12352–12359.
12. Young, L. S. 1984. The clinical challenge of infections due to *Pseudomonas aeruginosa. Rev. Infect. Dis.* 6:S603–S607.
13. Pier, G. B., G. J. Small, and H. B. Warren. 1990. Protection against mucoid *Pseudomonas aeruginosa* in rodent models of endobronchial infections. *Science* (Wash. DC). 249:537–540.
14. Gray, G. L., D. H. Smith, J. S. Baldridge, R. N. Harkins, M. L. Vasil, E. Y. Chen, and H. L. Heyneker. 1984. Cloning, nucleotide sequence, and expression in *Escherichia coli* of the exotoxin A structural gene of *Pseudomonas aeruginosa. Proc. Natl. Acad. Sci. USA.* 81:2645–2649.
15. Allured, V. S., R. J. Collier, S. F. Carroll, and D. B. McKay. 1986. Structure of exotoxin A of *Pseudomonas aeruginosa* at 3.0-Ångstrom resolution. *Proc. Natl. Acad. Sci. USA* 83:1320–1324.
16. Hwang, J., D. J. Fitzgerald, S. Adhya, and I. Pastan. 1987. Functional domains of *Pseudomonas* exotoxin identified by deletion analysis of the gene expressed in E. coli. *Cell.* 48:129–136.
17. Siegall, C. B., V. K. Chaudhary, D. J. FitzGerald, and I. Pastan. 1989. Functional analysis of domains II, Ib, and III of *Pseudomonas* exotoxin. *J. Biol. Chem.* 264:14256–14261.
18. Hwang, J., and M. S. Chen. 1989. Structure and function relationship of *Pseudomonas* exotoxin A. An immunochemical study. *J. Biol. Chem.* 264:2379–2384.
19. Zalman, L. S., and B. J. Wisnieski. 1984. Mechanism of insertion of diphtheria toxin: peptide entry and pore size determinations. *Proc. Natl. Acad. Sci. USA.* 81:3341–3345.
20. Zalman, L. S., and B. J. Wisnieski. 1985. Characterization of the insertion of *Pseudomonas* exotoxin A into membranes. *Infect. Immun.* 50:630–635.
21. Parker, M. W., A. D. Tucker, D. Tsernoglou, and F. Pattus. 1990. Insights into membrane insertion based on studies of colicins. *Trends Biochem. Sci.* 15:126–129.
22. Forti, S., and G. Menestrina. 1989. Staphylococcal alpha-toxin increases the permeability of lipid vesicles by a cholesterol and pH dependent assembly of oligomeric channels. *Eur. J. Biochem.* 181:767–773.
23. Menestrina, G., S. Forti, and F. Gambale. 1989. Interaction of tetanus toxin with lipid vesicles. Effects of pH, surface charge, and transmembrane potential on the kinetics of channel formation. *Biophys. J.* 55:393–405.
24. Gambale, F., and M. Montal. 1988. Characterization of the channel properties of tetanus toxin in planar lipid bilayers. *Biophys. J.* 53:771–783.
25. Bezanilla, F. 1985. A high capacity data recording device based on a digital audioprocessor and a video cassette recorder. *Biophys. J.* 47:437–441.
26. Pederzolli, C., L. Cescatti, and G. Menestrina. 1991. Chemical modification of *S. aureus* α-toxin by diethylpyrocarbonate: role of histidines in its membrane damaging properties. *J. Membr. Biol.* 119:41–52.
27. Laemmli, U. K. 1970. Cleavage of structural proteins during the assembly of the head of bacteriophage T4. *Nature (Lond.).* 227:680–685.
28. Farahbakhsh, Z. T., R. L. Baldwin, and B. J. Wisnieski. 1987.

Effect of low pH on the conformation of *Pseudomonas* exotoxin A. *J. Biol. Chem.* 262:2256–2261.

29. Sandvig, K., and J. Ø. Moskaug. 1987. *Pseudomonas* toxin binds Triton X-114 at low pH. *Biochem. J.* 245:899–901.
30. Zhao, J. M., and E. London. 1988. Localization of the active site of diphtheria toxin. *Biochemistry.* 27:3398–3403.
31. Cabiaux, V., M. Vandenbranden, P. Falmagne, and J. M. Ruysschaert. 1984. Diphtheria toxin induces fusion of small unilamellar vesicles at low pH. *Biochim. Biophys. Acta.* 775:31–36.
32. Papini, E., R. Colonna, F. Cusinato, C. Montecucco, M. Tomasi, and R. Rappuoli. 1987. Lipid interaction of diphtheria toxin and mutants with altered fragment B: liposome aggregation and fusion. *Eur. J. Biochem.* 169:629–635.
33. Schwarz, G. 1987. Basic kinetic of binding and incorporation with supramolecular aggregates. *Biophys. Chem.* 26:163–169.
34. Schwarz, G., H. Gerke, V. Rizzo, and S. Stankowsky. 1987. Incorporation kinetics in a membrane, studied with the pore-forming peptide alamethicin. *Biophys. J.* 52:685–692.
35. Wiegel, F. W. 1983. Diffusion and the physics of chemoreception. *Phys. Rep.* 95:283–319.
36. Farahbakhsh, Z. T., R. L. Baldwin, and B. J. Wisnieski. 1986. *Pseudomonas* exotoxin A. Membrane binding, insertion, and traversal. *J. Biol. Chem.* 261:11404–11408.
37. Miller, C. 1984. Ion channels in liposomes. *Annu. Rev. Physiol.* 46:449–458.
38. Defrise-Quertain, F., V. Cabiaux, M. Vandenbranden, R. Wattiez, P. Falmagne, and J. M. Ruysschaert. 1989. pH-dependent bilayer destabilization and fusion of phospholipidic large unilamellar vesicles induced by diphtheria toxin and its fragments A and B. *Biochemistry.* 28:3406–3413.
39. Falmagne, P., C. Capiau, V. Cabiaux, M. Deleers, and J.-M. Ruysschaert. 1984. Fragment B of diphtheria toxin: correlation between amino acid sequence and lipid binding properties. *In* Bacterial Protein Toxins. J. E. Alouf, F. J. Feherenbach, J. H. Freer, and J. Jeljaszewicz, editors. Academic Press, London. 139–146.
40. Parker, M. W., F. Pattus, A. D. Tucker, and D. Tsernoglou. 1989. Structure of the membrane-pore-forming fragment of colicin A. *Nature (Lond.).* 337:93–96.
41. Jiang, J. X., and E. London. 1990. Involvement of denaturation-like changes in *Pseudomonas* exotoxin A hydrophobicity and membrane penetration determined by characterization of pH and thermal transitions. Roles of two distinct conformationally altered states. *J. Biol. Chem.* 265:8636–8641.
42. Blewitt, M. G., L. A. Chung, and E. London. 1985. Effect of pH on the conformation of diphtheria toxin and its implications for membrane penetration. *Biochemistry.* 24:5458–5464.
43. Zhao, J. M., and E. London. 1988. Conformation and model membrane interactions of diphtheria toxin fragment A. *J. Biol. Chem.* 263:15369–15377.
44. Sigworth, F. J., and S. M. Sine. 1987. Data transformations for improved display and fitting of single-channel dwell time histograms. *Biophys. J.* 52:1047–1054.
45. Kyte, I., and R. F. Doolittle. 1982. A simple method of displaying the hydropathic character of a protein. *J. Mol. Biol.* 157:105–132.